doi: 10.1109/AUPEC48547.2019.211855

Battery Energy Storage System for Improving Primary Frequency Control with Increased Level of Photovoltaic Penetration

Ujjwal Datta
College of Engineering and Science
Victoria University
Victoria 8001, Melbourne, Australia
ujjwal.datta@live.vu.edu.au

Akhtar Kalam
College of Engineering and Science
Victoria University
Victoria 8001, Melbourne, Australia
akhtar.kalam@vu.edu.au

Juan Shi
College of Engineering and Science
Victoria University
Victoria 8001, Melbourne, Australia
juan.shi@vu.edu.au

***Abstract*—Power system inertia reduces with the increasing level of sustainable Photovoltaic (PV) generation. Hence, the power system will encounter several inevitable technical challenges, mainly in primary frequency control following a disturbance event. In this paper, a droop controlled Battery Energy Storage System (BESS) is proposed to reduce frequency oscillation by enhancing primary frequency controllability according to Australian National Energy Market (NEM) grid code and facilitate an increased level of PV penetration. Fossil-fueled based synchronous generator unit is replaced and the impact of PV penetration at various level is investigated. Moreover, battery state-of-charge recovery are also incorporated in this study. Simulation results with the droop-controlled BESS demonstrate that BESS effectively enhances the damping capability of the system in responding to primary frequency control and diminishes inertia related adverse impact with increased PV growth in the electric grid. In addition, it is observed that the system loading and generator control exhibit significant domination on primary frequency control of the system with the same level of PV penetration.**

***Index Terms*—Primary frequency control, Battery Energy Storage System, power oscillation, photovoltaic (PV) penetration level**

I. Introduction

The necessity of sustainable energy has given rise to the assimilation of renewable energy sources in power systems and the increased penetration level of renewable sources is expected in the near future. Although photovoltaic (PV) and wind energy sources are at the center of attention, the dynamic impact of PV energy system has not been investigated earlier due to their limited penetration level. Based on renewable electricity standards and present-day installation scenarios, PV is predicted to continue its strong growth in the coming years [1]. Therefore, with rapid growth in installed PV capacity, their impact can no longer be ignored and the detailed impact of PV is yet to be completely investigated.

With added PV capacity, the available inertia will be reduced which may affect negatively in dynamic and transient stability of the system. The study of small signal and transient stability analysis in [2], [3] shows that the increased penetration of PV increases frequency oscillations due to lower system inertia. However, authors in [4] demonstrated that system oscillations are well damped with distributed PV penetration, nevertheless positive impacts are subjected to fault location and the installation point of the distributed PV. With the adverse impacts of decreased inertia on power system stability, many research works have focused on the compensation of power imbalances by means of different control structure in PV plant. The authors in [5], [6] demonstrated that controlling PV power converters with a synchronous power controller provides better oscillation damping and reduces frequency deviation. The authors in [7] demonstrated that the improvement in oscillation damping can be achieved using a damping controller at PV plant based on wide area measurement. However, participating in such frequency stability requirements demand curtailed operation.

Very few studies have investigated the impact of auxiliary devices on damping out low frequency oscillation. Authors in [8] have shown that PV system with ultra-capacitor provides better oscillation damping than without ultra-capacitor. On the contrary, BESS has been acknowledged as one of the most prominent technologies in reducing fluctuations of intermittent PV energy [9], [10], alleviating transient frequency oscillation at different DG penetration levels [11] and regulating grid voltage with increased PV penetration [12]. An experimental study in [13] demonstrated that BESS is capable of responding within 80ms which is fast enough to provide fast primary frequency control response. Although BESS location with increased renewable penetration is proposed in [14], the impact of existing generator control and system loading is not considered in the presented study. Also, none of the above studies proposed any insight on state-of-charge (SOC) recovery strategy.

This paper investigates different level of PV penetration fol-

This work was supported by the Victoria University International Postgraduate Research Scholarship (IPRS) scheme.

lowing transient events that may potentially affect the primary frequency control of the system to maintain frequency oscillation within the mandatory grid requirements. A droop-controlled BESS is proposed in enhancing oscillation damping capability of the system and regulate output response of the system within the grid defined window. Multiple case studies have been carried out to demonstrate the efficacy of BESS in reducing negative impact of the increased PV penetration on primary frequency control by providing additional system damping. In addition, the domination of synchronous generator control and system loading on primary frequency response with increased PV penetration is also investigated. Furthermore, SOC recovery strategy is also presented to ensure BESS reliability to participate in future transient events.

II. Grid Requirements and Modeling of BESS

Generating units must maintain grid defined frequency range at any given time to ensure reliable grid operation and avoid possible system outage. The frequency operating boundary is governed by various factors such as the specific country grid codes, types of fault events and duration of faults. In this study, the considered frequency operating standards are according to Australian NEM. The non-critical frequency boundary is 0.997-1.003 pu whereas 0.99-1.01 p.u is the limit for load/generation events, 0.98-1.02 p.u for network event for the duration of 5 seconds and the frequency of generating units must not violate the above mentioned ranges at any circumstances [15]. The primary objective of incorporating BESS is to provide additional oscillation damping and satisfy grid operation following the above mentioned standards.
BESS is an arrangement of battery bank associated with a three-phase bi-directional converter and a step-up transformer coupled with the main grid. The very distinctive feature of BESS is its competency to regulate the active and reactive power individually as shown in Fig. 1. The active power input is limited by the available battery capacity whereas the total amount of reactive power is constrained by the bi-directional converter capacity. The active and reactive power is regulated by the individual current controllers on d and q axis. The general BESS design is described in different sections and those are elaborately described as follows:

A. Frequency Controller

The deviation between grid frequency and reference frequency generates active power signal. Then, BESS power varies according to the frequency droop characteristics [16] as shown in Fig. 2 to regulate BESS response and can be written as shown in (1)

$$\Delta f = \frac{1}{R_{BESS}}(f_{ref} - f_{grid}) \tag{1}$$

where, f_{ref} is the frequency reference (1 pu), and $1/R_{BESS}$ is the slope of the frequency droop. BESS discharges active power, if Δf is positive and the battery is charged if Δf is negative. The deadband defines the boundary to remain deactivated which is $\pm$ 0.003 per unit of the nominal frequency

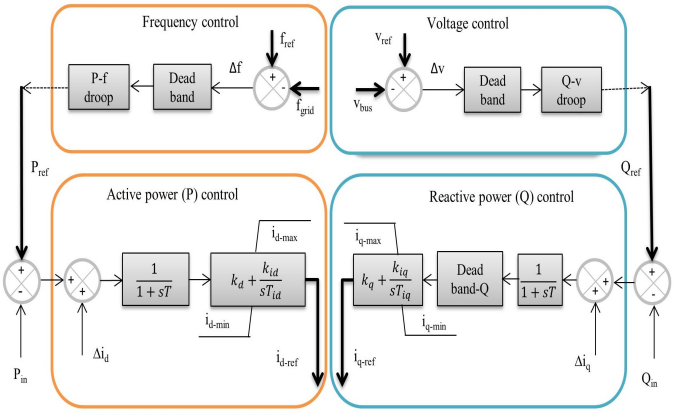

Fig. 1. The block diagram of the BESS active and reactive power control

value according to NEM. Active power control in Fig. 1 generates active current reference signal based on BESS droop characteristics.

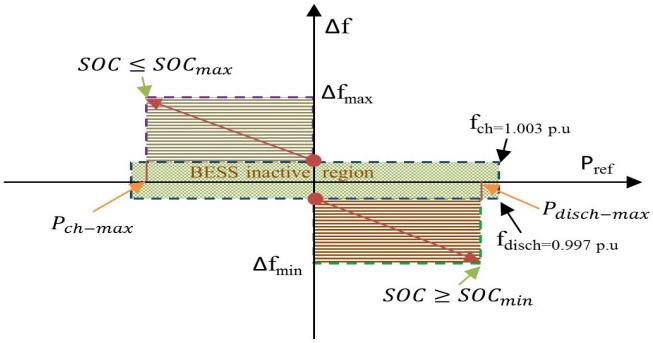

Fig. 2. Power-frequency droop characteristics

1) Voltage droop controller: The voltage controller initiates reactive power signal based on the imbalances between the actual and reference bus voltage as shown in Fig. 1 to control BESS response as shown in (2)

$$\Delta v = \frac{1}{R_{BESS}}(v_{ref} - v_{bus}) \tag{2}$$

where, v_{ref} is the voltage reference (pu) and $1/R_{BESS}$ is the slope of voltage droop. The BESS reactive power contribution depends on positive (supply) or negative (consume) value of Δv. The deadband value for voltage control is selected as 0.04 per unit of the nominal voltage value.

2) Active / Reactive Power (PQ) Controller: The active power (P) controller generates active power reference signal based on the active power error between P_{ref} and P_{in} and Δi_d from the charge controller, the first-order filter and a proportional-integral (PI) controller. The reactive power controller (Q) generates the reactive power reference signal considering reactive power error between Q_{ref} and Q_{in} and Δi_q from the charge controller, the first-order filter and the PI controller. The charge controller, d and q axis current controller are presented in Fig. 3.

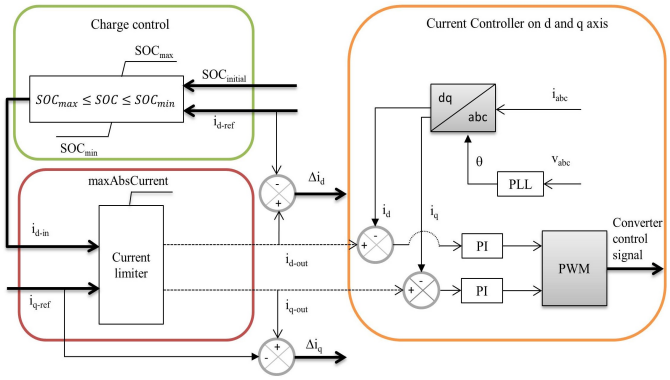

Fig. 3. The block diagram of the BESS Charge controller, d and q axis Current Control

$$y_o(s) = \left[K_p * y_{error}(s) + K_i \int_{y_{min}}^{y_{max}} \frac{1}{sT_i} * y_{error}(s) \right]_{y_{min}}^{y_{max}} \quad (3)$$

where, y_{error} is the error signal between BESS reference input and output. The controller is bounded by the maximum and minimum value and the parameters are tuned by Ziegler-Nichols method to reduce frequency undershoot (f_{nadir}), frequency overshoot (f_{max}) and settling time (t_{st}). The corresponding PI parameters are given in Appendix A.

B. BESS Charge Controller and Charging Management

Battery charging or discharging is controlled by battery state-of-charge (SOC) as shown in Fig. 3. There are mainly two different charging/discharging strategies which are presented in this study.

1) Droop Controlled Charging/Discharging: The basic droop-type charging/discharging control mechanism of the battery can be written as:

$$i_{d-in} = \begin{cases} i_{d-ref} & \text{if } SOC \geq SOC_{min} \\ -i_{d-ref} & \text{if } SOC \leq SOC_{max} \\ 0 & \text{if } SOC_{max} < SOC < SOC_{min} \end{cases}$$

BESS can supply active power as long as battery SOC is $\geq$ 0.2 pu (minimum SOC) and consume active power if SOC is $\leq$ 1 pu (maximum SOC). The active and reactive power references on d and q axis are limited by the maximum absolute current value of 1 per unit that defines the total capacity of BESS converter. The difference between the charge controller input and output of d axis current as Δi_d and q axis current as Δi_q is added in PQ controller to calculate the active and reactive power error.

2) SOC Recovery Strategy: The battery SOC changes while energy is exchanged in frequency regulation, therefore, battery should be recharged to ensure enough BESS capacity for future contingency events. On the contrary, it is also needed to assure that SOC level is kept to a level that BESS can take part in over-frequency event. Therefore, SOC recharging ceiling must be kept to a limit lower than the maximum SOC. Hence, the battery charging recovery can be written as:

$$i_{d-in} = \begin{cases} i_{ch-cur} & \text{if SOC} \leq 0.5 \text{ or SOC} \leq \text{SOC}_{min} \\ & \textit{and } i_{d-ref} < 0.0001 \\ 0 & \text{SOC}< \text{SOC}_{up-limit} \end{cases}$$

If SOC of the battery and the active power current reference is less than 0.5 p.u and 0.0001 pu respectively, the battery should be recharged until SOC reaches to the upper limit and this can be adjusted according to the planning of the BESS operator. The purpose of regulating the battery recharge threshold to be less than the maximum SOC is to advocate specific frequency reserve for over-frequency excursion.

C. dq Current Controller

The d and q axis current controller regulates BESS active and reactive power by adjusting d and q axis current using a PI controller. The feedback signal is the converters AC current in dq reference frame. The output signal of the d and q axis current controller is a pulse width modulated signal to control the DC/AC converter operation.

D. Battery Model

As an accurate modeling of chemical reaction based battery remains a challenging task, an equivalent electrical representation of a battery is considered as a common choice. The battery model used in this work is available in [17] where the battery is treated as a DC source with an internal resistance.

E. Step-up Transformer

Since the BESS AC terminal voltage is 0.4kV, a step-up transformer is required to connect BESS to the desired bus voltage of 230kV in the network.

III. Attributes of the Test System and Case Studies

A. Attributes of the Test System

PV penetration level and its impact are investigated on IEEE 9 bus system as shown in Fig. 4 [18]. The transient simulation studies are carried out in DigSILENT. The synchronous generators (SGs) are modeled as Hydro plant (G1), Gas turbine (G2) and Coal plant (G3) with associated turbines governor systems and automatic voltage regulator (AVR). The details of network modeling can be found in [19]. The SGs are considered to maintain a constant voltage at their local bus terminal. PV systems are installed at bus 9 via 0.6/230kV transformer and BESS are incorporated at bus 7. The detail modeling of PV system can be found in [20]. The PV systems are connected as an aggregated unit at bus 9 through a 0.4/230kV transformer. The notion of this study is to displace G3 unit and integrate more PV energy into the system. The BESS is connected to bus 7 via bi-directional DC/AC converter and a 0.4/230kV transformer to the grid.

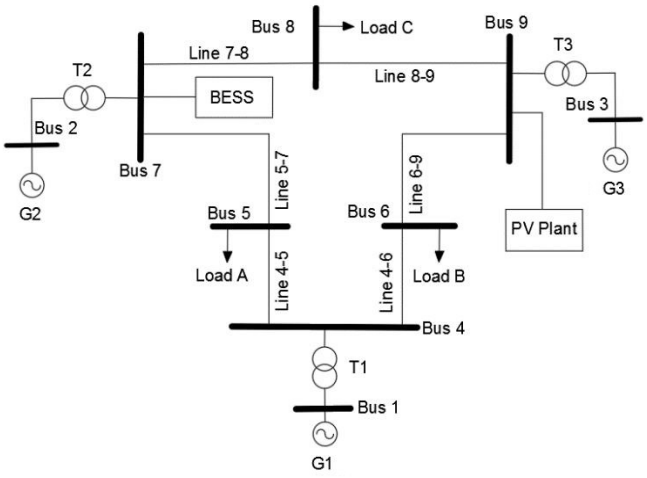

Fig. 4. The WSCC system with PV and BESS location

The representation of PV penetration is calculated as in (4):

$$\%PV_{penetration} = \frac{\sum P_{PV}}{\sum P_{PV} + \sum P_{SG}} \tag{4}$$

where, $\sum P_{PV}$ and $\sum P_{SG}$ is the total output power in MW from PV and SGs unit. There are two crucial aspects that determine PV penetration level and its impact on overall system inertia and they are as follows:

- Existing SG units remain in operation regardless of PV penetration level.
- Existing SG units are displaced with PV penetration.

B. Low and Heavy load Scenarios

The system responses are investigated at various levels of PV penetration with different loading conditions and the system loading distributions are given in Table I. PV penetration and the control of generator loading is also highlighted in the study to explore system performance in response to primary frequency control. Table II outlines two different operating strategies of the generator for low-load condition. In low-load condition, 150 MW PV generation is considered, whereas for heavy loaded scenario, both 75 MW and 150 MW PV generation are compared. Generator shares the total load demand nearly in equal manner (approximate loading of 47% by each generator with 150 MW PV and 60% with 75 MW PV). However, for low load case, different types of generating loading is selected to investigate the system performance at various generator loading conditions.

TABLE I
LOAD PROFILE (MW) IN DIFFERENT OPERATION MODES

Load type	Load A	Load B	Load C
Low load	125	90	100
Heavy load	175	110	115

TABLE II
GENERATOR OUTPUT AT DIFFERENT OPERATING STRATEGIES W/LOW LOAD

Strategy	G1 (MW)	G2 (MW)	PV (MW)
Strategy 1	100 (33.2%)	72 (29.3%)	150
Strategy 2	120 (40%)	53 (22.5%)	150

C. Case Studies

The level of PV penetration and its impact on power systems is mainly subjected to PV installation location along with the type and location of faults. To understand different aspects of PV penetration, four different case studies are considered with low load and heavy loaded condition:

- Case 1: Line outage with low load and generator control
- Case 2: Temporary and permanent line outage with heavy load
- Case 3: BESS Recharging

Strategy 1 defines 100MW PV penetration with nominal operation of synchronous generators whereas strategy 2 defines when generators are operated at uneven loading condition. The active power demand at low load is 315 MW and at heavy load is 400 MW. The increment of both generators output due to permanent load growth is reflected in heavy loaded scenario that replicates the circumstance when selecting convenient generator output option is not available to meet higher load demand.

IV. ANALYSIS OF TRANSIENT STABILITY

The rationale of transient analysis is to identify the impact of PV penetration level on power system output responses under various disturbance events. Simulations are carried out in DigSILENT for line outage, load events and PV output power reduction events at different PV penetration level. The main objective of the transient analysis is to recognize PV penetration impact on primary frequency control of the power system and the effectivenss of BESS in enhancing oscillation damping capability.

A. Line outage with low load and generator control strategies

The control of synchronous generator has significant influence on primary frequency response with PV penetration. Two different generator operating strategies are examined with low load and 150MW PV penetration. The individual generators' output at both strategies are outlined in Table II. The temporary line outage events are applied on line 2 for 0-0.25s and permanent line outage on line 6 from 0s onwards to observe damping capability of the system in primary frequency control. Simulation results in Fig. 5 illustrates that when the generators are operating with strategy 1, the output of the system oscillates within the defined grid operating frequency range.

However, generator G2 violates frequency requirements when operating with strategy 2 as G2 has lower available headroom compared to strategy 1. The output of the system exhibits enhanced performance with an integrated BESS at

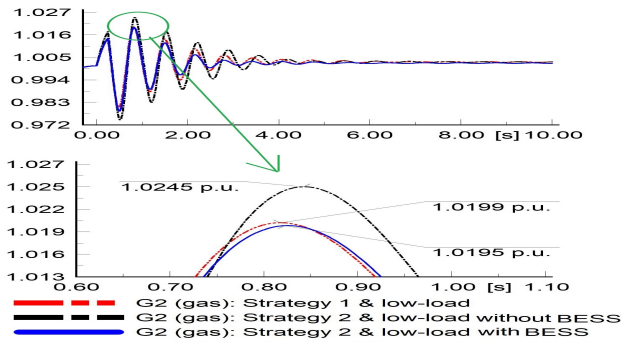

Fig. 5. The frequency of generator G2 [pu] with various operating strategies

bus 7 that complies with the grid requirements. Therefore, it is evident that sufficient power reserve in synchronous generator's terminal has significant contribution in improving primary frequency control of the system. Considering the perspective of primary frequency control, BESS can be an effective choice as such frequency control requires the maximum support for a short period of time only (several seconds).

B. Temporary and permanent line outage with heavy load

The aforementioned line fault events are applied at heavy loaded condition. The simulation results shown in Fig. 6 reflects that displacement of G3 and PV penetration reduces the damping potentiality of the system. The output illustrate that the system provides sufficient damping for line outage transients without any PV generation and with 75 MW PV generation. However, with 150 MW PV penetration, the system fails to provide similar damping support and eventually violates grid compatibility requirements as shown in Fig. 6. The generator G1 also exhibits similar response.

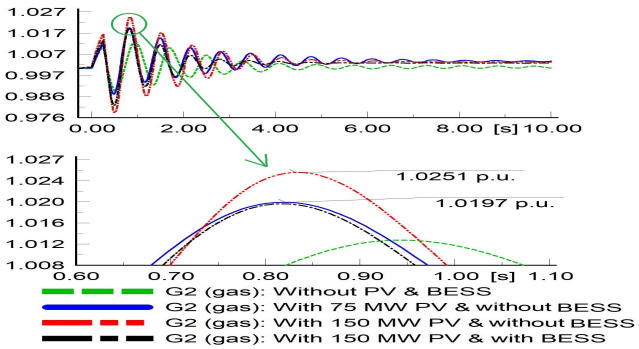

Fig. 6. The frequency of generator G2 [pu] with heavy load

Hence, a 20 MW (BESS converter size) BESS is incorporated at bus 7 to provide additional damping to the system and to enhance the damping capability of the system with increased level of PV penetration. It can be observed from Fig. 6 that BESS provides adequate damping to the system frequency and secures network performances according to the grid compatibility. It is worth noting that, even though generators have the capacity to feed total load demand, it loses efficiency in regulating primary frequency control that satisfies grid compatibility as PV penetration increases. Therefore, a smaller BESS installed in the grid can potentially improve system performance for the required period of time and conveniently facilitate further PV penetration with a modest size.

The voltage response at BESS connection point shown in Fig. 7 demonstrates that BESS improves the voltage profile when the system encounters transients and also the system stabilizes at a faster rate than without a BESS. It also can be observed in Fig. 8 that BESS significantly contributes in reducing active power oscillations of generator compared to the case without a BESS. The generator G1 also shows similar level of improved performance with BESS.

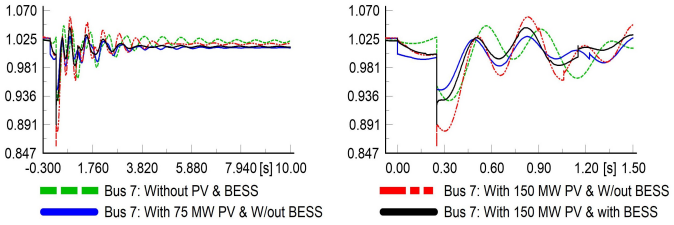

Fig. 7. Voltage [pu] at BESS connection point

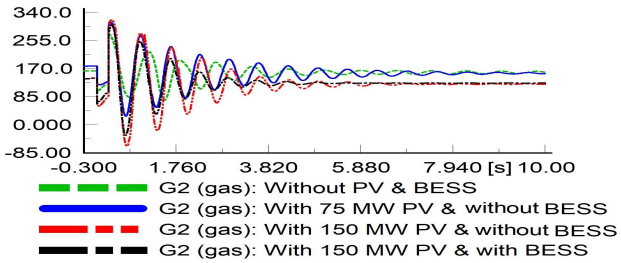

Fig. 8. Active power output [MW] of generator G2

BESS active and reactive power exchange during transient periods are shown in Fig. 9. The maximum amount of active and reactive power of BESS are 20 MW and 15 MVar. The battery SOC changes very slowly depending on energy surplus and shortfall as shown in Fig. 9 that advocates the efficacy of smaller BESS size for enhanced system response.

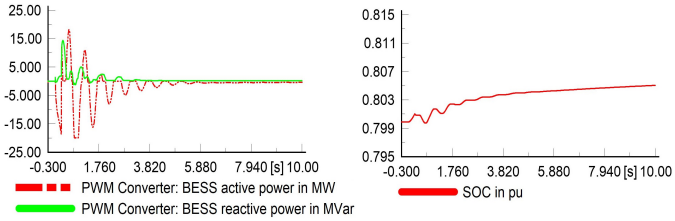

Fig. 9. BESS active and reactive power

C. BESS Recharging

Battery SOC changes due to the exchange of BESS power with the grid and also self-discharging characteristics of the

battery. Therefore, SOC recharging facility is required to ensure battery is charged enough to participate in exchanging power whenever it is needed. The proposed SOC recovery strategy is demonstrated in Fig. 10. The results illustrate the efficacy of the proposed SOC recovery strategy. Figure 10

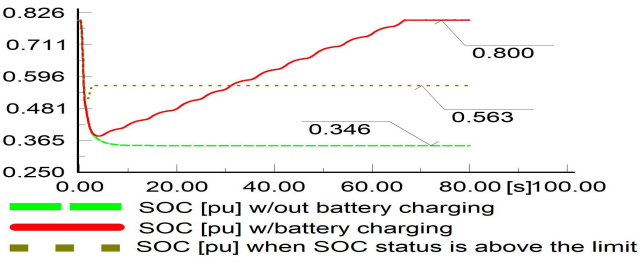

Fig. 10. Battery recharging scenarios

shows that without SOC recovery charging current, SOC reduces to 0.346 pu. According to the design, the battery is charged to the defined recharging limit with a recharging current of 0.035 pu. It is worth noting that, this defined SOC recharging ceiling doesn't affect the droop-type charging limit of the maximum SOC. It is also observed that when battery SOC stays at a value higher than the designed 0.5 pu value, SOC recovery charging action remains inactive and this validates the proper functioning of the proposed SOC recovery strategy.

V. Conclusion

In this study, a droop controlled BESS is incorporated in a medium size transmission system to enhance system damping capability in primary frequency control and diminish negative inertial impact of increased PV penetration. The simulation results demonstrate that BESS provides sufficient damping and enhances the capability of providing primary frequency control with respect to power mismatches in the system resulting from contingency phenomena. It is perceived with 30% PV penetration, power grid fails to provide the required damping for primary frequency control following the grid compatibility. A small size of BESS is found to ensures the affinity of the frequency responses according to the grid requirements. In addition, BESS reduces active power and voltage oscillations at a faster rate than a system without a BESS. Simulation results also illustrate the efficacy of the proposed charging strategy to recover SOC at various operating point.

Future works will focus on increasing PV penetration level, dynamic load characteristics and the control of energy storage system in the vicinity of stability enhancement.

Appendix

Battery Parameters: Initial SOC=0.8 pu, battery cell capacity=20 Ah, series cells=10, parallel cells= 65, nominal source voltage= 0.9kV, internal resistance=0.001 ohm.
PI controller (in pu): d-axis (T=0.01, K_d=K_{id}1.5, T_{id}=0.01, i_{d-min}=-1, i_{d-max}=1), q-axis (T=0.02, K_q=K_{iq}2, T_{iq}=0.05, i_{q-min}=-1, i_{q-max}=1), Deadband-Q=0.01

References

[1] International Energy Agency, "Renewables 2017, [Available Online]: https://www.iea.org/publications/renewables2017, [Accessed on: 2018-07-01]."

[2] S. You, G. Kou, Y. Liu, X. Zhang, Y. Cui, M. J. Till, W. Yao, and Y. Liu, "Impact of high PV penetration on the inter-area oscillations in the U.S. eastern interconnection," *IEEE Access*, vol. 5, pp. 4361–4369, 2017.

[3] S. You, Y. Liu, X. Zhang, Y. Su, L. Wu, Y. Liu, and S. W. Hadley, "Impact of high PV penetration on U.S. eastern interconnection frequency response," in *2017 IEEE Power Energy Society General Meeting*, Jul 2017, pp. 1–5.

[4] S. Eftekharnejad, V. Vittal, G. T. Heydt, B. Keel, and J. Loehr, "Impact of increased penetration of photovoltaic generation on power systems," *IEEE Transactions on Power Systems*, vol. 28, no. 2, pp. 893–901, May 2013.

[5] D. Remon, A. M. Cantarellas, J. M. Mauricio, and P. Rodriguez, "Power system stability analysis under increasing penetration of photovoltaic power plants with synchronous power controllers," *IET Renewable Power Generation*, vol. 11, no. 6, pp. 733–741, 2017.

[6] D. Remon, C. A. Caizares, and P. Rodriguez, "Impact of 100-MW-scale PV plants with synchronous power controllers on power system stability in northern chile," *IET Generation, Transmission Distribution*, vol. 11, no. 11, pp. 2958–2964, 2017.

[7] R. Shah, N. Mithulananthan, and K. Y. Lee, "Large-scale PV plant with a robust controller considering power oscillation damping," *IEEE Transactions on Energy Conversion*, vol. 28, no. 1, pp. 106–116, Mar 2013.

[8] Q. Sun, Z. Xiao, J. Fan, F. Wang, S. Chen, and Y. Zhai, "Influences of secondary arc-based grading capacitor of multi-break circuit breaker on the transient stability of power system," *International Journal of Electrical Power & Energy Systems*, vol. 107, pp. 577 – 588, 2019.

[9] M. J. E. Alam, K. M. Muttaqi, and D. Sutanto, "A novel approach for ramp-rate control of solar pv using energy storage to mitigate output fluctuations caused by cloud passing," *IEEE Transactions on Energy Conversion*, vol. 29, no. 2, pp. 507–518, June 2014.

[10] P. M. Ariyaratna, K. M. Muttaqi, and D. Sutanto, "The simultaneous mitigation of slow and fast voltage fluctuations caused by rooftop solar pv by controlling the charging/discharging of an integrated battery energy storage system," *Journal of Energy Storage*, vol. 26, p. 100971, 2019.

[11] A. K. Srivastava, A. A. Kumar, and N. N. Schulz, "Impact of distributed generations with energy storage devices on the electric grid," *IEEE Systems Journal*, vol. 6, no. 1, pp. 110–117, March 2012.

[12] J. Krata and T. K. Saha, "Real-time coordinated voltage support with battery energy storage in a distribution grid equipped with medium-scale pv generation," *IEEE Transactions on Smart Grid*, vol. 10, no. 3, pp. 3486–3497, May 2019.

[13] D. Greenwood, K. Lim, C. Patsios, P. Lyons, Y. Lim, and P. Taylor, "Frequency response services designed for energy storage," *Applied Energy*, vol. 203, pp. 115 – 127, 2017.

[14] M. Ramrez, R. Castellanos, G. Caldern, and O. Malik, "Placement and sizing of battery energy storage for primary frequency control in an isolated section of the mexican power system," *Electric Power Systems Research*, vol. 160, pp. 142 – 150, 2018.

[15] AEMC, "The Frequency Operating Standard stage one final-for-publi, [Available Online]: https://www.aemc.gov.au/sites/default/files/content/ce48ba94-b3a9-4991-9ef9-e05814a78526/REL0065-Review-of-the-Frequency-Operating-Standard-Final-for-publi.pdf, [Accessed on: 2018-07-15]."

[16] S. Akkari, J. Dai, M. Petit, and X. Guillaud, "Interaction between the voltage-droop and the frequency-droop control for multi-terminal HVDC systems," *IET Generation, Transmission Distribution*, vol. 10, no. 6, pp. 1345–1352, 2016.

[17] M. Chen and G. A. Rincon-Mora, "Accurate electrical battery model capable of predicting runtime and I-V performance," *IEEE Transactions on Energy Conversion*, vol. 21, no. 2, pp. 504–511, June 2006.

[18] P. M. Anderson and A. A. Fouad, *Power System Control and Stability, 2nd Edition*. New York: IEEE Press, 2003.

[19] DigSILENT, "Digsilent Powerfactory," 2017.

[20] DigSILENT GmbH, "PV system," 2017.